AIAA JOURNAL
Vol. 30, No. 10, October 1992

# Generalized Compound Scaling Algorithm and Application to Minimum Weight Design of Plate Structures

Ramana V. Grandhi* and Narayana S. Venugopal†
*Wright State University, Dayton, Ohio 45435*
and
Vipperla B. Venkayya‡
*Wright Laboratory, Wright Patterson Air Force Base, Ohio 45433*

**This paper presents the generalized compound scaling algorithm and its application to optimum weight design of plate structures. The optimum designs are reached by simply scaling the design variables to an optimum intersection of multiple constraints. A four-noded isoparametric plate element is used for modeling the structure. Sensitivity computations and the optimization algorithm are discussed. The optimization cost involved (excluding the finite element analyses) is very small using this algorithm. The procedure is demonstrated on three example problems using stress and displacement constraints with side bounds on the design variables.**

## Introduction

In the past 20 years optimality criteria methods (OCM) have been successfully applied in the design of large-scale structural optimization problems.[1-3] The success of OCM is largely attributed to the application of an active constraint strategy where the number of active constraints in each cycle is limited to a small subset of the total constraints. This subset is updated in each cycle, and the strategy allows the new constraints to enter while others leave. The OCM presented in Ref. 1 consisted of two basic steps referred to as resizing and scaling. Both are iterative in the design space, and their purpose is to search for the optimum. The resizing algorithm is used when the design is on the constraint surface with respect to one or more active constraints. It is derived directly from the optimality conditions. The scaling step, on the other hand, is to bring the design to the constraint surface when it is away from the boundary. When the constraints and the objective are linear functions of the variables, the scaling to the constraint surface can be accomplished in a single step. Based on this premise, the OCM method was applied to design a number of large-scale aerospace structures with stress, displacement, and frequency constraints.[1-5] Because of the perceived limitation of the scaling step, previous applications of OCM were limited to structures modeled with membrane elements (trusses and wings).

Generalization of the scaling to linear and nonlinear functions is a major advance in the application of OCM to a wide variety of mathematical optimization problems.[6] The derivation in Ref. 6 considered both membrane and bending structures with stress, displacement, and frequency constraints. The development of the compound scaling algorithm constitutes further generalization to include multiple constraints. The compound scaling finds constraint intersections (Fig. 1). The nonlinear optimization algorithm presented in Ref. 7 uses the idea of compound scaling to solve the entire optimization problem by appending the objective function to the constraint set. This requires generation of pseudotargets for the objective function. This idea is intriguing because it opens the idea of extending compound scaling to multicriteria optimization.

The purpose of this paper is to present the generalized compound scaling (GCS) algorithm and to demonstrate it on plate structures optimization. In these problems, the stiffness matrix of the bending elements is a nonlinear function of the design variables.

Haftka and Prasad[8] documented well the previous work done on structural optimization of plate bending elements. From the literature, it was observed that the number of plate structures optimized using finite element models is very limited. This may be because of the complexity of the element formulation, the sensitivity analysis, and the associated optimization issues. Selected publications of the previous work are discussed next.

Erbatur and Mengi[9] used the principle of stationary mutual potential energy in the design of circular plates under a rotational load using a deflection constraint. Armand and Lodier[10] used a single displacement constraint based optimality criteria in designing plate structures. The authors considered triangular bending elements for modeling the simply supported and clamped plates. Based on the optimum material distributions, the authors concluded that, wherever there was the most material located along some curves, those were the potential locations for placing ribs or stiffeners. Prasad and Haftka[11] studied plate structure optimization using a cubic extended penalty function approach. Though this approach gave good convergence, it proved to be computationally expensive for very large-order problems. Fleury et al.[12] employed primal and dual formulations by incorporating efficient constraint approxima-

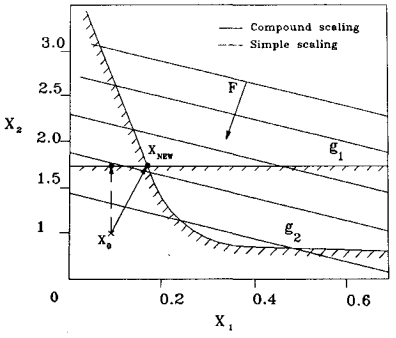


**Fig. 1 Demonstration of compound scaling technique.**

Presented as Paper 91-0923 at the AIAA/ASME/ASCE/AHS/ASC 32nd Structures, Structural Dynamics, and Materials Conference, Baltimore, MD, April 8-10, 1991; received July 31, 1991; revision received March 9, 1992; accepted for publication March 24, 1992. 

*Associate Professor, Department of Mechanical and Materials Engineering.
†Graduate Research Assistant, Department of Mechanical and Materials Engineering.
‡Wright Laboratory Fellow.

tion concepts for optimizing plate bending problems. Lin and Yang[13] used Lagrangian multipliers and Kuhn-Tucker conditions along with scaling to optimize plate structures modeled with an eight-noded isoparametric element. Moore and Vanderplaats[14] used the force approximation method for shape design of plate structures.

In the present study, the generalized compound scaling algorithm is used along with a four-noded isoparametric plate element. The optimum results are achieved without using any resizing algorithm, hence avoiding the anamolies involved with Lagrangian multipliers. In this paper the element formulation, sensitivity analysis, and generalized compound scaling algorithm are discussed. Three plate structures are optimized with stress and displacement constraints by considering up to 100 design variables and more than 300 constraints.

## Sensitivity Analysis

A four-noded isoparametric plate element was used in this work. The formulation of this element is presented in the Appendix. Sensitivity analysis for plate elements was discussed by Brockman and Lung.[15] The authors used a single point integration for all of the components of the stiffness matrix. A stabilization matrix was used to overcome singularity problems. In the present study, the formulation was carried out with $2 \times 2$ integration for membrane and bending components whereas a choice is given for the transverse shear terms as to whether to use either a $1 \times 1$ or a $2 \times 2$ integration. This was necessary because of the loss of accuracy during the optimization process where the element thicknesses vary considerably among the adjacent elements.

In the present study, the element formulation was carried out with the sensitivity in mind. The membrane, bending, and shear part of the stiffness matrices were computed separately, which enabled the differentiation of these matrices explicitly. Three matrices $K_m$, $K_b$, and $K_s$ are computed separately, and they are differentiated for the computation of $\partial K/\partial t$, where $t$ is the plate element thickness. The $K_m$ and $K_s$ vary linearly with thickness whereas $K_b$ has a cubic relation with thickness. Hence, for each element,

$$\left[\frac{\partial K}{\partial t}\right] = \begin{bmatrix} \frac{1}{t}[K_m] & 0 \\ 0 & \frac{3}{t}[K_b] + \frac{1}{t}[K_s] \end{bmatrix} \tag{1}$$

The matrices $K_m$, $K_b$, and $K_s$ are computed and stored without the $t$ terms. Then these matrices are differentiated independently and added.

The static equilibrium equation for the structure is

$$[K]\{u\} = \{P\} \tag{2}$$

where $u$ is the displacement vector and $P$ is the applied load vector.

Differentiation of the previous equation with respect to the element thickness yields

$$\left\{\frac{\partial u}{\partial t_i}\right\} = [K]^{-1}\left[-\frac{\partial K}{\partial t_i}\right]\{u\} \tag{3}$$

In the previous equation, only $\partial K/\partial t$ is computed and multiplied with element displacements. The product is then expanded as the global pseudoload vector. This is because, while differentiating $K$ with respect to $t_i$, only the contribution from $K_i$ are nonzero.

In the computation of stress constraint sensitivity, the separation of membrane, bending, and shear parts are again carried out.

From the plate element formulation, the stresses are computed as

$$\{\sigma_j\} = \int [D_j][B_j]\{u_j\}\, dv_j \tag{4}$$

where $D$ is the material matrix, $B$ is the strain-displacement matrix, and $v_j$ is the volume of the element.

Differentiation of the previous equation yields

$$\left\{\frac{\partial \sigma_j}{\partial t_i}\right\} = \int [D_j][B_j]\left\{\frac{\partial u_j}{\partial t_i}\right\} + \int \left[\frac{\partial D_j}{\partial t_i}\right][B_j]\{u_j\} \tag{5}$$

Similar to the stress computation, the membrane, bending, and shear components of $\partial \sigma_j/\partial t_i$ are computed separately and added. It can be observed that the second part of Eq. (5) vanishes if $i \neq j$.

## Optimization Algorithm

One of the most challenging problems in structural optimization with finite element models is the ability to handle large-order systems with numerous design variables and constraints. As the order of the system increases, both the response and the sensitivity analyses require excessive computer resources. GCS is a computationally efficient approach for optimization of an objective function subject to multiple constraints. The major advantage of this technique is that it is possible to optimize problems with thousands of variables and constraints. The computational cost is minimal because of the reduced number of operations involved in reaching the optimum by using the response and sensitivity derivatives information.

In the present work, the GCS algorithm is used in solving the complete optimization problem. A strategy was incorporated into the algorithm to decrease the objective function while scaling without resorting to any resizing approach. This avoided the computation of Lagrangian multipliers. Figure 1 shows the differences in simple and compound scaling techniques. In compound scaling, constraint intersections are identified while minimizing the objective function.

The constrained optimization problem is stated as follows:

Minimize the structural weight $F(x)$ subject to the behavior constraints

$$g_j(x) \leq \bar{g}_j \qquad j = 1, 2, \ldots, p \tag{6a}$$

$$g_j(x) = \bar{g}_j \qquad j = p+1, \ldots, m \tag{6b}$$

and side constraints

$$x^{\ell} \leq x \leq x^{u} \tag{7}$$

where $x_i$ are the element thicknesses, and $g_j$ and $\bar{g}_j$ are the constraints and the constraint bounds, respectively. In the present study, constraints are placed on displacements and stresses; $n$ and $m$ are the number of variables and constraints, respectively. Lower and upper limits on the variables are given in Eq. (7), where the superscripts $\ell$ and $u$ represent the lower and upper limits, respectively.

## Generalized Compound Scaling

Important steps involved in the GCS algorithm are given in Fig. 2 as a flow chart, and the mathematical details of these steps are given next. Two simple parameters $\beta$ and $\mu$ play a key role in the generalized compound scaling.

The $\beta$ parameters are computed for all of the constraints using the following expression:

$$\beta_j = \frac{\bar{g}_j}{g_j} = \text{target response ratio} \tag{8}$$

A small subset of constraints with the lowest values of $\beta$ are selected for compound scaling and are denoted by $s$. Next, the function characteristic parameter $\mu$ is computed for each of the $s$ constraints. The $\mu$ parameter consists of two parts as given next.

For all negative $\mu_{ij}$ terms:

$$\mu_{jN} = -\sum_{i=1}^{n} \mu_{ij} \qquad j = 1, 2, \ldots, s \tag{9}$$

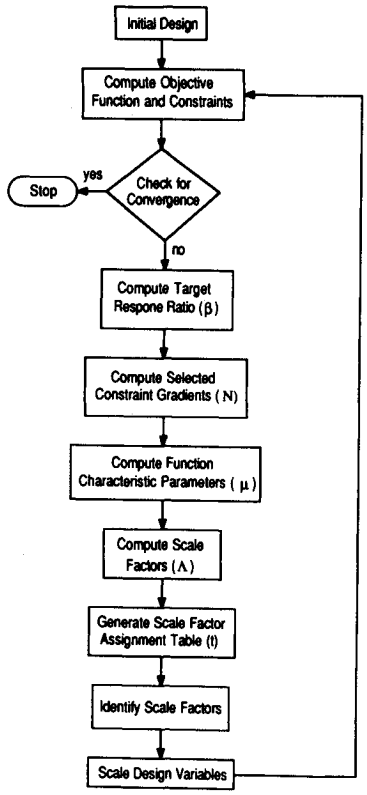


**Fig. 2 Generalized compound scaling algorithm flow chart.**

For all positive $\mu_{ij}$ terms:

$$\mu_{jP} = \sum_{i=1}^{n} \mu_{ij} \qquad j = 1, 2, \ldots, s \tag{10}$$

where

$$\mu_{ij} = \frac{N_{ij} x_i}{g_j} \tag{11}$$

and where $N_{ij}$ is the gradient of the $j$th constraint function with respect to the $i$th variable:

$$N_{ij} = \frac{\partial g_j}{\partial x_i} \tag{12}$$

The $\beta$ and $\mu$ parameters are also computed for the objective function using similar procedures as described next.

For all negative $\mu_{iF}$ terms:

$$\mu_{FN} = -\sum_{i=1}^{n} \mu_{iF} \tag{13}$$

For all positive $\mu_{iF}$ terms:

$$\mu_{FP} = \sum_{i=1}^{n} \mu_{iF} \tag{14}$$

where

$$\mu_{iF} = \left(\frac{\partial F}{\partial x_i} x_i\right) \Big/ F \tag{15}$$

The $\beta_F$ is computed using a pseudotarget function:

$$\beta_F = \frac{1 + \alpha\beta_{\min}}{1 + \alpha} \qquad \mu_{FN} \geq \mu_{FP} \tag{16a}$$

$$= \frac{1}{\beta_F} \qquad \mu_{FN} < \mu_{FP} \tag{16b}$$

where $\beta_{\min}$ is the smallest $\beta$ value, and $\alpha$ is computed using the largest $\mu$ value information:

$$\alpha = \mu_{jN} \qquad \mu_{jN} \geq \mu_{jP} \tag{17a}$$

$$= \frac{1}{\mu_{jP}} \qquad \mu_{jN} < \mu_{jP} \tag{17b}$$

Scale factors $\Lambda$ are computed using the values of the function characteristic parameters and target response ratios. The procedure is as follows:

$$\Lambda_{jN} = \left(\frac{1}{\beta_j}\right)^{1/\mu_{jN}} \qquad \mu_{jN} \geq \mu_{jP} \tag{18}$$

or

$$\Lambda_{jP} = (\beta_j)^{1/\mu_{jN}} \qquad \mu_{jN} < \mu_{jP} \tag{19}$$

Similar expressions are also used for the objective function with appropriate information. The entries in each column of the scale factors matrix can have two possible values. For example, when $\mu_{jN} \geq \mu_{jP}$, the $j$th column of the matrix will have $\Lambda_{jN}$ values corresponding to all of the terms that contributed to the sum in Eq. (9) and 1.0 for the terms contributing to the sum in Eq. (10). Similarly, in the case when $\mu_{jN} < \mu_{jP}$, the entries contributing to the sum in Eq. (10) will have $\Lambda_{jP}$ and the remaining 1.0. In summary, the following conditions are used in constructing the scale factors matrix:

$$\left.\begin{aligned} \Lambda_{ij} &= \Lambda_{jN} \qquad \mu_{ij} < 0 \\ \Lambda_{ij} &= 1.0 \qquad \mu_{ij} \geq 0 \end{aligned}\right\} \qquad \mu_{jN} \geq \mu_{jP} \tag{20a}$$

or

$$\left.\begin{aligned} \Lambda_{ij} &= \Lambda_{jP} \qquad \mu_{ij} > 0 \\ \Lambda_{ij} &= 1.0 \qquad \mu_{ij} \leq 0 \end{aligned}\right\} \qquad \mu_{jN} < \mu_{jP} \tag{20b}$$

The same strategy is used in building the $s + 1$ column for the objective function. This formulation results in possible $s + 1$ scale factors for each variable. Which one of the $s + 1$ scale factors is relevant to the given variable is determined with the help of a scale factor assignment procedure.

The format of the scale factor assignment matrix $t_{ij}$ ($n$ by $s + 1$) is similar to the scale factor matrix. The elements $t_{ij}$ are calculated as follows:

$$\left.\begin{aligned} t_{ij} &= \left|\frac{N_{ij} x_i}{g_j}\right| \div \mu_{jN} \qquad \mu_{ij} < 0 \\ t_{ij} &= 0 \qquad \mu_{ij} \geq 0 \end{aligned}\right\} \qquad \mu_{jN} \geq \mu_{jP} \tag{21a}$$

or

$$\left.\begin{aligned} t_{ij} &= \left|\frac{N_{ij} x_i}{g_j}\right| \div \mu_{jP} \qquad \mu_{ij} > 0 \\ t_{ij} &= 0 \qquad \mu_{ij} \leq 0 \end{aligned}\right\} \qquad \mu_{jN} < \mu_{jP} \tag{21b}$$

The $s + 1$ column for the objective function is computed as follows:

$$t_{ij} = \left|\left(\frac{\partial F}{\partial x_i} x_i\right) \Big/ F\right| \div \mu_{FN} \qquad \mu_{FN} \geq \mu_{FP} \tag{22a}$$

or

$$t_{ij} = \left|\left(\frac{\partial F}{\partial x_i} x_i\right) \Big/ F\right| \div \mu_{FP} \qquad \mu_{FN} < \mu_{FP} \tag{22b}$$

It is important to note that $g_j$ is not allowed to be negative because the $\beta$ value is not allowed to be negative in view of its

participation in the exponential formula for the scale factors [Eqs. (18) and (19)].

Now all of the information is available for the selection of an appropriate scale factor for each variable from the list of $s + 1$ scale factors. An appropriate scale factor for the $i$th variable is selected based on the following principles:

1) From the scale factor assignment matrix, select the largest entry in the $i$th row. For example, if $t_{ij}$ is the largest entry in the scale factor assignment matrix, then the appropriate scale factor for the $i$th variable is the $\Lambda_{ij}$ from the scale factor matrix.

2) If there is more than one entry equal to the largest entry in that row, then the appropriate scale factor corresponds to the smallest $\beta_j$ of the equal entries.

Now this process of selecting an appropriate scale factor is applied for all of the variables. The selected scale factor for the $i$th variable is denoted by $r_i$. The scaled variables for $x_i$ are computed by

$$x_i^{\text{new}} = r_i x_i^{\text{old}} \qquad i = 1, 2, \ldots, n \tag{23}$$

The compound scaling algorithm simply drives the design to the intersection of the constraints if such an intersection exists. Additional details of the optimization strategy are given in Ref. 7.

## Numerical Results and Discussions

### Example 1: Cantilever Beam with Multiple Load Conditions

A beam of 10 in. length and 1 in. width was optimized for minimum weight (Fig. 3). The material properties were

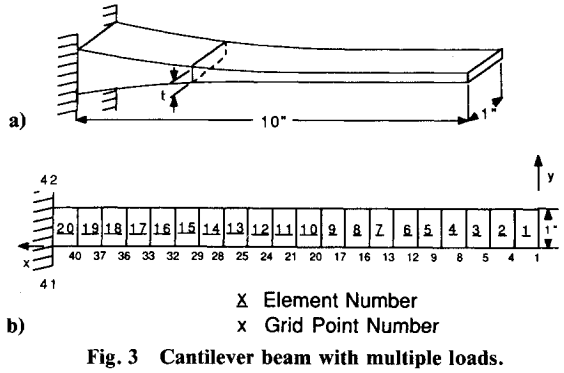


**Fig. 3 Cantilever beam with multiple loads.**

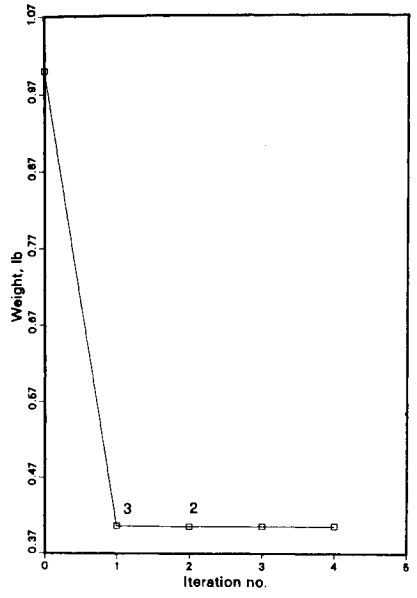


**Fig. 4 Cantilever beam design iteration history.**

**Table 1 Optimal design for cantilever beam**

| Element no. | Thickness |
|---|---|
| 1 | 0.3000 |
| 2 | 0.3000 |
| 3 | 0.3006 |
| 4 | 0.3006 |
| 5 | 0.4309 |
| 6 | 0.4309 |
| 7 | 0.4309 |
| 8 | 0.4309 |
| 9 | 0.4309 |
| 10 | 0.4309 |
| 11 | 0.4309 |
| 12 | 0.4309 |
| 13 | 0.4309 |
| 14 | 0.4309 |
| 15 | 0.4309 |
| 16 | 0.4309 |
| 17 | 0.4309 |
| 18 | 0.4309 |
| 19 | 0.4309 |
| 20 | 0.4414 |

Initial weight, 1.000 lb. Final weight, 0.405 lb.

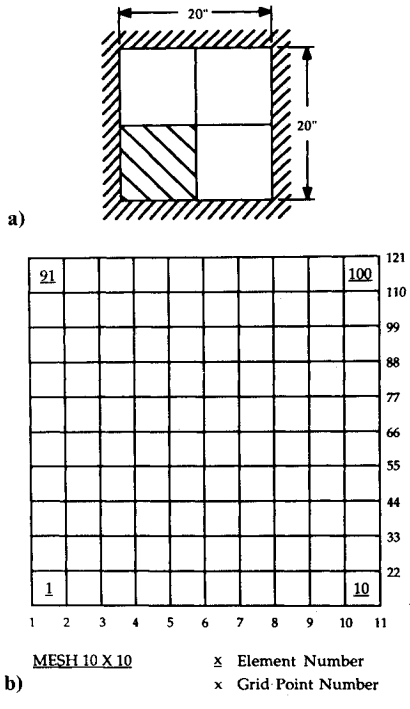


**Fig. 5 Clamped square plate with uniform lateral load.**

$E = 10^7$ psi, $\nu = 0.3$, and $\rho = 0.1$ lb/in.$^3$. The beam was subjected to multiple load conditions: 1) an end moment of 450 lb-in. and 2) a tip load of 100 lb.

This problem was solved earlier for the first load condition by Haug and Kirmser[16] using an analytical approach and later by Prasad and Haftka[11] using the finite element method. Prasad and Haftka used a cubic extended penalty function approach for the optimization. The mesh used in the present study is the same as the mesh used in Ref. 11.

The beam was modeled with 20 elements as a $20 \times 1$ mesh. A total of 20 design variables (thicknesses of all of the elements) and 164 constraints for normal stresses and displacements under the aforementioned two load conditions were considered in the optimization. The allowable normal stress was 30,000 psi. It was required that the tip deflection be limited to 0.5 in. The minimum thickness allowed was 0.1 in.

At the initial design, all of the thicknesses were chosen to be 1.0 in., which is in the feasible region. The initial structural

weight was 1.0 lb. An optimal design of 0.4053 lb was obtained with eight finite element analyses. The iteration history of the feasible designs is given in Fig. 4 by indicating the number of finite element analyses involved from the previous design. The optimal design is given in Table 1. At the optimal design, the stress constraints at the free end element under the first load case reached the limit. In the second load case, the free end displacement as well as stress on the two elements near the clamped end reached the constraint boundary. The thickness was the highest at the cantilevered end and the lowest at the free end.

The analysis results at the initial and optimal designs were compared with NASTRAN. The differences were less than 1% in both displacements and stresses.

**Example 2: Square Plate Clamped at the Edges**

A square plate clamped at the edges (Fig. 5) is the next example case. It was subjected to a uniform lateral load of 16 psi. The plate dimensions were $20 \times 20$ in. Only a quarter of the plate was considered due to symmetry. This problem was earlier solved by Lin and Yang[13] using an eight-noded plate element with a $5 \times 5$ mesh. In the present study, a $10 \times 10$ mesh of four-noded isoparametric plate element was used. The material properties were $E = 1.05 \times 10^7$ psi, $\nu = 0.3$, and $\rho = 0.1$ lb/in.$^3$. The maximum allowable normal stress was 12,000 psi. It was required that the deflection at all of the points of the plate be restricted to 0.1 in. The minimum thickness allowed was 0.03937 in.

The initial design (infeasible) had an uniform thickness of 0.03937 in. for all of the elements (an initial weight of 0.3937 lb). A total of 100 design variables and 321 constraints were considered. An optimal design of 2.679 lb was obtained with 31 analyses. Figure 6 presents the iteration history for the feasible designs. The optimal design is given in Table 2, and the distribution of design variables is shown in Fig. 7.

At the optimal design, the deflections at the nodes 110, 120, and 121 were active. Higher values of stresses for $\sigma_x$ occurred in the elements near the clamped edge of the top left corner of the quarter model, whereas $\sigma_y$ had higher values near the bottom right corner of the clamped edge.

**Table 2 Optimal design for clamped square plate**

| Element no. | Thickness | Element no. | Thickness |
|---|---|---|---|
| 1 | 0.0420 | 35, 44 | 0.3696 |
| 2, 11 | 0.0420 | 36, 54 | 0.3518 |
| 3, 21 | 0.0420 | 37, 64 | 0.3518 |
| 4, 31 | 0.0606 | 38, 74 | 0.0394 |
| 5, 41 | 0.3907 | 39, 84 | 0.0394 |
| 6, 51 | 0.3907 | 40, 94 | 0.0394 |
| 7, 61 | 0.3652 | 45 | 0.3696 |
| 8, 71 | 0.3644 | 46, 55 | 0.3518 |
| 9, 81 | 0.3662 | 47, 65 | 0.3484 |
| 10, 91 | 0.3652 | 48, 75 | 0.3001 |
| 12 | 0.0420 | 49, 85 | 0.0394 |
| 13, 22 | 0.0420 | 50, 95 | 0.0394 |
| 14, 32 | 0.0899 | 56 | 0.3518 |
| 15, 42 | 0.4511 | 57, 66 | 0.3038 |
| 16, 52 | 0.3984 | 58, 76 | 0.3038 |
| 17, 62 | 0.3334 | 59, 86 | 0.3690 |
| 18, 72 | 0.3579 | 60, 96 | 0.3579 |
| 19, 82 | 0.3088 | 67 | 0.3414 |
| 20, 92 | 0.3373 | 68, 77 | 0.3038 |
| 23 | 0.0583 | 69, 87 | 0.3001 |
| 24, 33 | 0.0583 | 70, 97 | 0.3001 |
| 25, 43 | 0.3518 | 78 | 0.3213 |
| 26, 53 | 0.3518 | 79, 88 | 0.3154 |
| 27, 63 | 0.3297 | 80, 98 | 0.3001 |
| 28, 73 | 0.3038 | 89 | 0.3213 |
| 29, 83 | 0.3038 | 90, 99 | 0.3351 |
| 30, 93 | 0.2327 | 100 | 0.3491 |
| 34 | 0.3643 | | |

Initial design, 0.393 lb (infeasible). Final design, 2.679 lb.

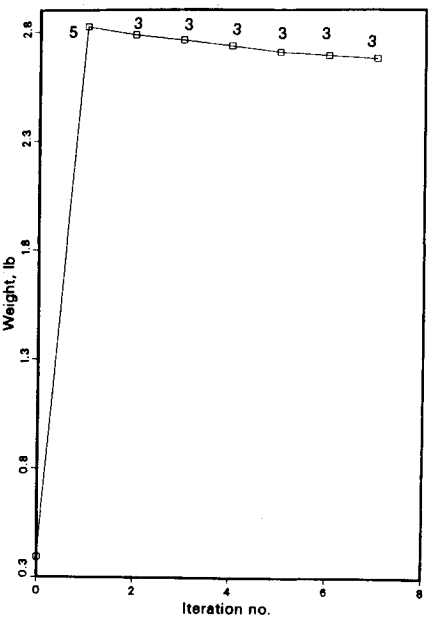


**Fig. 6 Clamped square plate design iteration history.**

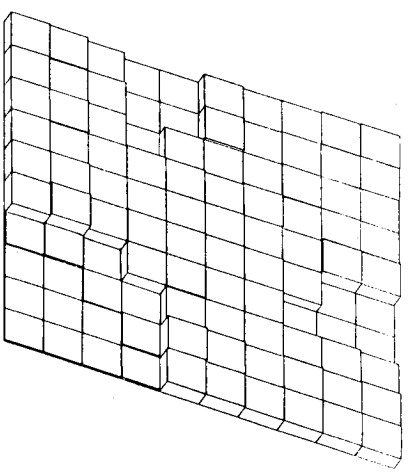

**Fig. 7 Clamped square plate optimal thickness distribution.**

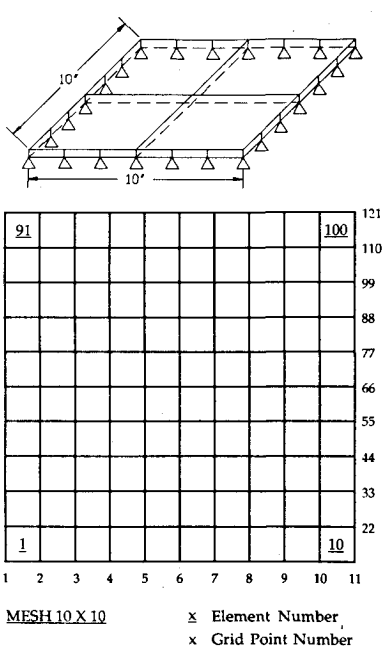


**Fig. 8 Simply supported square plate with multiple loads.**

**Table 3 Optimal design for clamped square plate**

| Element no. | Thickness | Element no. | Thickness |
|---|---|---|---|
| 1 | 0.7736 | 51 | 0.1470 |
| 2 | 0.7736 | 52 | 0.2350 |
| 3 | 0.1470 | 53 | 0.2350 |
| 4 | 0.1470 | 54 | 0.2867 |
| 5 | 0.1470 | 55 | 0.2723 |
| 6 | 0.1470 | 56 | 0.1958 |
| 7 | 0.1470 | 57 | 0.4674 |
| 8 | 0.1470 | 58 | 0.2080 |
| 9 | 0.9800 | 59 | 0.1701 |
| 10 | 0.9800 | 60 | 0.1470 |
| 11 | 0.5310 | 61 | 0.1470 |
| 12 | 0.7073 | 62 | 0.2030 |
| 13 | 0.5477 | 63 | 0.2882 |
| 14 | 0.1958 | 64 | 0.2530 |
| 15 | 0.2001 | 65 | 0.2548 |
| 16 | 0.2066 | 66 | 0.2819 |
| 17 | 0.1958 | 67 | 0.3750 |
| 18 | 0.7073 | 68 | 0.2535 |
| 19 | 0.9800 | 69 | 0.1701 |
| 20 | 0.5250 | 70 | 0.1622 |
| 21 | 0.1470 | 71 | 0.1470 |
| 22 | 0.6074 | 72 | 0.1767 |
| 23 | 0.2075 | 73 | 0.2938 |
| 24 | 0.2075 | 74 | 0.1939 |
| 25 | 0.2112 | 75 | 0.2383 |
| 26 | 0.1976 | 76 | 0.1939 |
| 27 | 0.2093 | 77 | 0.3950 |
| 28 | 0.2189 | 78 | 0.1470 |
| 29 | 0.2949 | 79 | 0.1474 |
| 30 | 0.1701 | 80 | 0.1701 |
| 31 | 0.1470 | 81 | 0.4051 |
| 32 | 0.1470 | 82 | 0.4204 |
| 33 | 0.2190 | 83 | 0.2433 |
| 34 | 0.2539 | 84 | 0.1845 |
| 35 | 0.3001 | 85 | 0.1832 |
| 36 | 0.2808 | 86 | 0.1845 |
| 37 | 0.2093 | 87 | 0.2433 |
| 38 | 0.2823 | 88 | 0.2052 |
| 39 | 0.1711 | 89 | 0.1470 |
| 40 | 0.1547 | 90 | 0.1474 |
| 41 | 0.1470 | 91 | 0.3984 |
| 42 | 0.2633 | 92 | 0.3984 |
| 43 | 0.3092 | 93 | 0.2397 |
| 44 | 0.2618 | 94 | 0.1832 |
| 45 | 0.2547 | 95 | 0.1470 |
| 46 | 0.2762 | 96 | 0.1609 |
| 47 | 0.2931 | 97 | 0.1832 |
| 48 | 0.3894 | 98 | 0.2416 |
| 49 | 0.1547 | 99 | 0.2533 |
| 50 | 0.1470 | 100 | 0.2791 |

Initial weight, 10.000 lb. Final weight, 2.803 lb.

The analysis results at the initial and optimal designs were compared with NASTRAN. At the initial design, the maximum displacement had a difference of 2%, and at the optimal design, it was about 4%. The stresses have less than 1% difference at the initial and optimal designs. In this example, the $2 \times 2$ integration for transverse shear strains yielded unsatisfactory results compared with the $1 \times 1$ integration at the optimal design. The results presented were obtained using a $1 \times 1$ integration.

**Example 3: Simply Supported Square Plate**

A square plate simply supported at the edges (Fig. 8) is the final example. The $10 \times 10$ in. plate was subjected to multiple load conditions: 1) a uniform lateral load of 200 psi on the bottom two quadrants, and 2) a uniform lateral load of 133.33 psi on the bottom two and the upper left quadrants. The structure was modeled with 100 elements, and 642 design constraints and 100 design variables were considered in the optimization. The material properties were $E = 10^7$ psi, $\nu = 0.3$, and $\rho = 0.1$ lb/in.$^3$. The maximum allowable normal

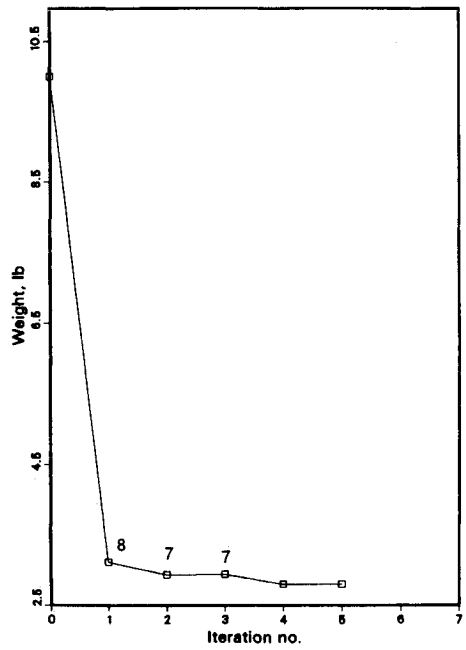


**Fig. 9 Simply supported plate design iteration history.**

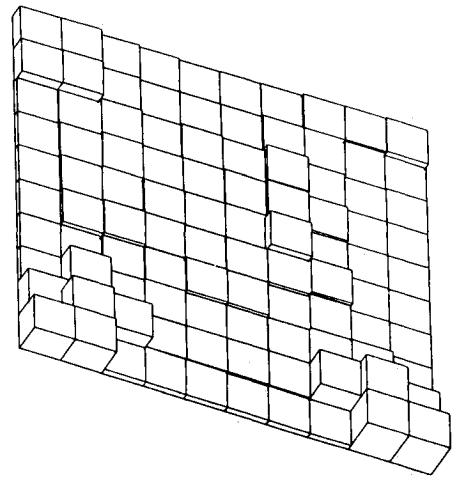

**Fig. 10 Simply supported square plate optimal thickness distribution.**

stress was 30,000 psi. It was required that the deflection at all of the points of the plate be restricted to 0.2 in. The minimum thickness allowed was 0.1 in.

The initial design had an uniform thickness of 1.0 in. and an initial weight of 10.0 lb. This design was in the feasible region. An optimal design of 2.803 lb was obtained by using 27 functional analyses, and Fig. 9 presents the design iteration history. The optimal design variables are listed in Table 3, and the design variables distribution is shown in Fig. 10. The optimum design was driven by stress constraints, and the displacement constraints were inactive.

The analysis results at the initial and optimal designs were verified using NASTRAN. At the initial design, the differences were less than 1%. At the optimal design, a difference of 3% in the maximum displacement and 4% in the maximum stress were observed.

## Summary

This paper presented the generalized compound scaling algorithm for solving the complete optimization problem. By scaling alone, the objective function was minimized for plate structures. The implementation of the algorithm is very simple and suitable for solving any general mathematical optimiza-

tion problem. In this work the methodology is applied to bending type problems, where the element stiffness is a nonlinear function of design variables. It was observed that the computational effort involved in the optimization part is very minimal.

In all of the problems, 10 constraints were considered in the active constraint set $s$ for the compound scaling. The active constraints were updated in each cycle. A maximum of 10 active constraints were retained, irrespective of the total number of constraints considered in the problem from the beginning of the optimization until the end. This algorithm reduced the computational cost of sensitivity analysis substantially as the design progressed closer to the optimum where generally a large number of constraints become active. The optimum designs reached with this methodology have about 5–10% higher objective function values compared with the available results. Finally, the algorithm presented in this paper can be used for multiobjective optimization problems by simply adding extra columns in scale factors and assignment table matrices.

## Appendix: Plate Element Formulation

The plate element formulation was carried out as given by Hughes.[17] The element stiffness matrix consists of three parts, namely, membrane, bending, and shear components, which are computed independently. This makes the computation of $\partial K/\partial t$ simpler:

$$[K_e] = \begin{bmatrix} K_m & 0 \\ 0 & K_b + K_s \end{bmatrix} \tag{A1}$$

where $K_e$ is the element stiffness matrix: $K_m$, $K_b$, and $K_s$ are the membrane, bending, and shear components of $K_e$:

$$[K_m] = \int [B_m]^T [D_m][B_m]\, dv \tag{A2}$$

where $B_m$ is the strain-displacement matrix and $D_m$ is the stress-strain matrix for the plane-stress analysis:

$$[B_m] = \begin{bmatrix} \frac{\partial N_1}{\partial x} & 0 & \frac{\partial N_2}{\partial x} & 0 & \frac{\partial N_3}{\partial x} & 0 & \frac{\partial N_4}{\partial x} & 0 \\ 0 & \frac{\partial N_1}{\partial y} & 0 & \frac{\partial N_2}{\partial y} & 0 & \frac{\partial N_3}{\partial y} & 0 & \frac{\partial N_4}{\partial y} \\ \frac{\partial N_1}{\partial y} & \frac{\partial N_1}{\partial x} & \frac{\partial N_2}{\partial y} & \frac{\partial N_2}{\partial x} & \frac{\partial N_3}{\partial y} & \frac{\partial N_3}{\partial x} & \frac{\partial N_4}{\partial y} & \frac{\partial N_4}{\partial x} \end{bmatrix} \tag{A3}$$

$$[D_m] = \frac{Et}{(1-\nu^2)} \begin{bmatrix} 1 & \nu & 0 \\ \nu & 1 & 0 \\ 0 & 0 & \frac{1-\nu}{2} \end{bmatrix} \tag{A4}$$

similarly,

$$[K_b] = \int [B_b]^T [D_b][B_b]\, dv \tag{A5}$$

$$[K_s] = \int [B_s]^T [D_s][B_s]\, dv \tag{A6}$$

$$[B_b] = \begin{bmatrix} 0 & -\frac{\partial N_1}{\partial x} & 0 & -\frac{\partial N_2}{\partial x} & 0 & -\frac{\partial N_3}{\partial x} & 0 & -\frac{\partial N_4}{\partial x} \\ \frac{\partial N_1}{\partial y} & 0 & \frac{\partial N_2}{\partial y} & 0 & \frac{\partial N_3}{\partial y} & 0 & \frac{\partial N_4}{\partial y} & 0 \\ \frac{\partial N_1}{\partial x} & -\frac{\partial N_1}{\partial y} & \frac{\partial N_2}{\partial x} & -\frac{\partial N_2}{\partial y} & \frac{\partial N_3}{\partial x} & -\frac{\partial N_3}{\partial y} & \frac{\partial N_4}{\partial x} & -\frac{\partial N_4}{\partial y} \end{bmatrix} \tag{A7}$$

$$[D_b] = \frac{t^2}{12}[D_m] \tag{A8}$$

$$[B_s] = \begin{bmatrix} \frac{\partial N_1}{\partial x} & 0 & N_1 & \frac{\partial N_2}{\partial x} & 0 & N_2 & \frac{\partial N_3}{\partial x} & 0 & N_3 & \frac{\partial N_4}{\partial x} & 0 & N_4 \\ \frac{\partial N_1}{\partial y} & -N_1 & 0 & \frac{\partial N_2}{\partial x} & -N_2 & 0 & \frac{\partial N_3}{\partial x} & -N_3 & 0 & \frac{\partial N_4}{\partial y} & -N_4 & 0 \end{bmatrix} \tag{A9}$$

$$[D_s] = \left(\frac{5}{6}\right) \frac{Et}{2(1+\nu)} \begin{bmatrix} 1 & 0 \\ 0 & 1 \end{bmatrix} \tag{A10}$$

In the case of $K_m$ and $K_b$, a $2 \times 2$ Gaussian integration was used. Reduced integration of $1 \times 1$ was used for $K_s$. In some cases the $1 \times 1$ integration for $K_s$ caused instability in the analysis results during the optimization process. In those cases, the transverse shear strains were computed as discussed by Hughes and Tezduyar.[18] This approach achieves quadratic accuracy with respect to Kirchhoff modes[17] and resulted in a $2 \times 2$ integration for the shear terms.

Again, in the case of stress computation, the three components, namely, membrane, bending, and shear, are computed separately and added:

$$\{\sigma\} = \{\sigma_m\} + \{\sigma_b\} + \{\sigma_s\} \tag{A11}$$

where

$$\{\sigma_m\} = [D_m][B_m]\{u_m\} \tag{A12}$$

$$\{\sigma_b\} = \frac{6}{t^2}[D_b][B_b]\{u_b\} \tag{A13}$$

$$\{\sigma_s\} = \frac{1}{t}[D_s][B_s]\{u_s\} \tag{A14}$$

where $u_m$, $u_b$, and $u_s$ are the nodal degrees of freedom:

$$\{u_m\} = \begin{Bmatrix} u \\ v \end{Bmatrix}, \quad \{u_b\} = \begin{Bmatrix} \theta_x \\ \theta_y \end{Bmatrix}, \quad \{u_s\} = \begin{Bmatrix} w \\ \theta_x \\ \theta_y \end{Bmatrix} \tag{A15}$$

## Acknowledgments

The research effort of the first two authors was supported by the U.S. Air Force through Contract F33615-88-C-3204. The authors acknowledge Geetha Bharatram for her assistance in generating the computer results.

## References

[1]Venkayya, V. B., "Design of Optimum Structures," *Journal of Computers and Structures,* Vol. 1, 1971, pp. 265–309.

[2]Berke, L., and Khot, N. S., "Use of Optimality Criteria Methods for Large Scale Systems," *Structural Optimization,* AGARD Lecture Series, No. 70, 1974.

[3]Gellatly, R. A., Helenbrook, R. G., and Kocher, L. H., "Multiple Constraints in Structural Optimization," *International Journal for Numerical Methods in Engineering,* Vol. 13, No. 2, 1978, pp.

297-310.

[4]Grandhi, R. V., and Venkayya, V. B., "Structural Optimization with Frequency Constraints," *AIAA Journal,* Vol. 26, No. 7, 1988, pp. 858-866.

[5]Canfield, R. A., Grandhi, R. V., and Venkayya, V. B., "Structural Optimization with Stiffness and Frequency Constraints," *Journal of Mechanics of Structures and Machines,* Vol. 17, No. 1, 1989, pp. 95-110.

[6]Venkayya, V. B., "Optimality Criteria: A Basis for Multidisciplinary Design Optimization," *Journal of Computational Mechanics,* Vol. 5, 1989, pp. 1-21.

[7]Venkayya, V. B., "Design Optimization in Dynamic Environment," International Conference on Recent Advances in Structural Dynamics, Southhampton, England, UK, July 1991.

[8]Haftka, R. T., and Prasad, P., "Optimum Structural Design with Plate Bending Elements—A Survey," *AIAA Journal,* Vol. 19, No. 4, 1981, pp. 517-522.

[9]Erbatur, F., and Mengi, Y., "On Optimal Design of Plates for a Given Deflection," *Journal of Optimization Theory and Applications,* Vol. 21, No. 1, 1977, pp. 103-110.

[10]Armand, J. L., and Lodier, B., "Optimal Design of Bending Elements," *International Journal for Numerical Methods in Engineering,* Vol. 13, 1978, pp. 373-394.

[11]Prasad, B., and Haftka, R. T., "Optimum Structural Design with Plate Bending Finite Elements," *ASCE Journal of Structures Division,* Vol. 105, ST11, 1979, pp. 2367-2382.

[12]Fleury, C., Ramanathan, R. K., Salama, M., and Schmit, L. A., "ACCESS Computer Program for the Synthesis of Large Structural Systems," *New Directions in Optimum Structural Design,* edited by E. Atrek et al., Wiley, New York, 1984, pp. 541-561.

[13]Lin, C., and Yang, T., "Application of Multiplier Update Method to the Minimum Weight Design of Elastic Plates," *Journal of Computers and Structures,* Vol. 29, No. 6, 1988, pp. 943-948.

[14]Moore, G., and Vanderplaats, G. N., "Improved Approximations for Static Stress Constraints," *Proceedings of the AIAA/ASME/ASCE/AHS/ASC Structures, Structural Dynamics, and Materials Conference,* CP902, AIAA, Washington, DC, 1990, pp. 161-170 (AIAA Paper 90-1008).

[15]Brockman, R. A., and Lung, F. Y., "Sensitivity Analysis with Plate and Shell Finite Elements," *International Journal for Numerical Methods in Engineering,* Vol. 26, No. 5, 1988, pp. 1129-1143.

[16]Haug, E. J., and Kirmser, P. G., "Minimum Weight Design of Beams with Inequality Constraints on Stress and Deflection," *ASME Journal of Applied Mechanics,* Dec. 1967, pp. 999-1004.

[17]Hughes, T. J. R., *The Finite Element Method,* Prentice-Hall, Englewood Cliffs, NJ, 1987.

[18]Hughes, T. J. R., and Tezduyar, T. E., "Finite Elements Based Upon Mindlin Plate Theory with Particular Reference to the Four-node Bilinear Isoparametric Element," *ASME Journal of Applied Mechanics,* Vol. 48, 1981, pp. 587-596.